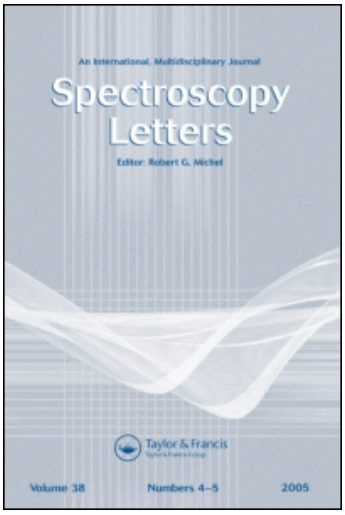

Spectroscopy Letters
Publication details, including instructions for authors and subscription information:
http://www.informaworld.com/smpp/title~content=t713597299

Study of the d-f Emission, and f-d Ground-State and Excited-State Absorption of Nd^{3+} in Crystals Using the Simple Model

Chang-Kui Duan[a]; Sha Jiang[a]
[a] Institute of Modern Physics, Chongqing University of Post and Telecommunications, Chongqing, P.R. China

Online publication date: 30 July 2010

To cite this Article Duan, Chang-Kui and Jiang, Sha(2010) 'Study of the d-f Emission, and f-d Ground-State and Excited-State Absorption of Nd^{3+} in Crystals Using the Simple Model', Spectroscopy Letters, 43: 5, 423 — 430
To link to this Article: DOI: 10.1080/00387010.2010.487022
URL: http://dx.doi.org/10.1080/00387010.2010.487022

Spectroscopy Letters, 43:423–430, 2010

ISSN: 0038-7010 print/1532-2289 online
DOI: 10.1080/00387010.2010.487022

Taylor & Francis
Taylor & Francis Group

Study of the d-f Emission, and f-d Ground-State and Excited-State Absorption of Nd^{3+} in Crystals Using the Simple Model

Chang-Kui Duan and Sha Jiang

Institute of Modern Physics, Chongqing University of Post and Telecommunications, Chongqing, P.R. China

ABSTRACT The simplified model for 4f-5d transitions is applied to obtain the line strengths for emission, ground-state absorption and excited states absorption involving 4f-5d transitions of Nd^{3+} in crystals. The results are host independent for the usual case where 5d crystal-field interaction can be considered as strong, in the sense that the calculated 5d-4f emission relative line strengths will be the same for Nd^{3+} in any host. Also the calculated 4f-5d absorption line strengths can be grouped by the 5d crystal-field components. For each 5d crystal-field component, the group of absorption line strengths for different $4f^2$5d transition final states forms a pattern independent of the 5d crystal-field component and the host. For practical cases, due to strong but still limited 5d crystal-field splitting, the transitions to different 5d crystal-field components may overlap each other. The theoretical results are used to interpret available experimental data.

KEYWORDS f–d transition, Nd^{3+}, excited–state absorption, crystal–field interaction, $LiYF_4$, YPO_4

INTRODUCTION

Due to applications or potential applications in UV and VUV lasers, scintillators, and quantum cutting phosphors, there have been tremendous studies of f-d transitions of trivalent lanthanide ions.[1–3] Systematic experimental studies of the $4f^N$- $4f^{N-1}$5d excitation and $4f^{N-1}$5d-$4f^N$ emission and theoretical modeling of energy-level patterns and transition intensities have been carried out for many systems.[4–6] Most measured spectra consist of several broad bands for 4f → 5d or 5d → 4f transitions and so this does not allow the determination of all the parameters in the extended crystal-field phenomenological Hamiltonian for the $4f^{N-1}$5d configuration. Therefore a simple model using 3–4 parameters has been developed by Duan et al.[7] and further extended to more sophisticated cases by Ning et al.,[8] Xia et al.,[9–12] Duan et al.[13] and Ma et al.[14] Another approach to deal with the spectra is to calculate the energy levels and transitions intensities using *ab initio* methods.[3,15] The available theoretical methods can usually simulate the measured spectra reasonably well, but the interpretation of the assignment of the measured peaks are usually lacking.

Received 2 October 2009; accepted 14 November 2009.

Address correspondence to Chang-Kui Duan, Institute of Modern Physics, Chongqing University of Post and Telecommunications, Chongqing 400065, P.R. China. E-mail: duanck73@hotmail.com

In this paper, it is shown, using Nd^{3+} as an example, that the 4f-5d ground and excited state absorptions and 5d-4f emissions can all be rationalized using the simple model, and the results are host independent for the usual case where the 5d crystal-field splitting is stronger than the 4f-5d Coulomb and 4f spin-orbit interactions. The results are then applied to interpret the 4f-5d ground-state and excited-state absorptions, and 5d-4f emissions for Nd^{3+} in various crystals. The bands in measured spectra are assigned and interpreted.

THEORY

For the purpose of d-f and f-d transitions, since the bands are usually broader than the splitting due to 4f crystal-field interactions, the quasi free ion Hamiltonian can be used to predict the relative energies of the multiplets for the $4f^N$ configuration and the $4f^{N-1}$ core. The Hamiltonian can be written as (detailed explanations are given in Liu[1]):

$$H = E_{\text{avg}} + \sum_{k=2,4,6} F^k \mathbf{f}_k + \zeta_{4f} \sum_i \mathbf{s}_i \cdot \mathbf{l}_i + \sum_{k=2-4,6-8} T^k \mathbf{t}_k(\text{f}) + \alpha \mathbf{L}^2(\text{f}) + \beta \mathbf{G}(G_2(\text{f})) + \gamma \mathbf{G}(G_7(\text{f})) + \sum_{k=0,2,4} M^k \mathbf{m}_k(\text{f}) + \sum_{k=2,4,6} P^k \mathbf{p}_k(\text{f}) \quad (1)$$

Here E_{avg} is a parameter to adjust the overall position of the configuration so as to align the lowest energy level at $0\,\text{cm}^{-1}$. F^k and ζ_{4f} are the most important parameters in determining the energy level structure of the $4f^N$ free ion or the $4f^{N-1}$ core and the wave functions of multiplets $^{2S+1}L_J$, which are subject to minor adjustment due to other correlation interactions and spin-other-orbit interactions. These quasi-free ion parameters vary from crystals to crystals slightly but actually differ substantially from the free ion values. Thus we adopt the mean quasi-free ion values from Gorller-Walrand and Binnemans[16] rather than the values for the free ions. It is also noted that the value of a particular parameter (such as ζ_{4f}) is expected to be different for $4f^N$ and the $4f^{N-1}$ core due to the contraction of radial distribution of 4f and other atomic orbitals *etc*. Experimental data are usually not sufficient to determine the values for the $4f^{N-1}$ core parameters and *ab initio* calculations tend to greatly overestimate them. It is expected that the $4f^N$ to $4f^{N-1}$ ratios for those parameters obtained from *ab initio* calculations are more accurate than the absolute values for those parameters and the ratios for F^k and ζ_{4f} parameters are readily available from Reid et al.[17] Those ratios are used to obtain the corresponding parameters for $4f^{N-1}$ core from $4f^N$. Other minor parameters for the $4f^{N-1}$ core are set to be the same as those for $4f^N$.

For the $4f^{N-1}5d$ configuration, apart from the interactions within the $4f^{N-1}$ core, there are the crystal-field interaction for 5d orbitals, and the 4f-5d Coulomb interaction. These are very important. The 5d spin-orbit interaction is usually less important.[8] The crystal-field interaction for 5d orbitals results into the splitting of 5d orbitals into crystal-field components, which are denoted as 5d Γ_i hereafter. The $4f^{N-1}$ core is split by 4f-4f Coulomb interaction into spectrum terms $4f^{N-1}(S_f L_f)$. Each $4f^{N-1}(S_f L_f)$ (5d Γ_i) is then split further by exchange part of the 4f-5d Coulomb interaction into high spin states $S = S_f + 1/2$ and low spin states $S = S_f - 1/2$. This exchange interaction is usually bigger than the 4f spin-orbit interaction for light lanthanide ions. Hence for each 5d Γ_i, the $(S_f s_{5d})S\, L_f\, J$ coupling is preferred instead of $(S_f L_f)J_f\ s_{5d}\ J$ or other couplings.[8] So we introduce the multiplet for $4f^{N-1}5d$ as

$$\left|^{2S+1}(4f^{N-1}\,\eta\,^{2S_f+1}L_f, 5d\,^2\Gamma_i)_J\right\rangle = \sum_{J_f} \left|(4f^{N-1}\eta(^{2S_f+1}L_f)_{J_f}, 5d\,^2\Gamma_i)_J\right\rangle \left\langle \left(\frac{1}{2}, (S_f, L_f)J_f\right)J \middle| \left(\frac{1}{2}, (S_f)S, L_f\right)J \right\rangle, \quad (2)$$

where S_f, L_f is the spin and orbit angular moment quantum number for the $4f^{N-1}$ core, respectively; $S = S_f \pm 1/2$ is the total spin for $4f^{N-1}5d$ configuration; Γ_i is the ith crystal-field component of 5d orbital with point-group irrep Γ_i, whose degeneracy is denoted as $[\Gamma_i]$, and J is the coupling of total spin S and orbit angular moment L_f (excluding the orbit angular moment of 5d). The multiplet is expanded in terms of the $(S_f L_f)J_f\ s_{5d}\ J$ coupling. The recoupling coefficients can be given in terms of 6*j* symbols but we calculate them here directly instead.

By following the approximation for the Coulomb interaction given in Ning et al.:[8]

$$H_{\text{coul}}(\text{fd}) = -J_{\text{ex}}\widehat{\mathbf{S}}_{\text{f}} \cdot \widehat{\mathbf{s}}_{\text{d}}, \tag{3}$$

we can write the energy for the multiplet $\left|^{2S+1}(4f^{N-1}\eta\,^{2S_f+1}L_f, 5d\,^2\Gamma_i)_J\right\rangle$ as follows:

$$\begin{aligned}
&E(\left|^{2S+1}(4f^{N-1}\eta\,^{2S_f+1}L_f, 5d\,^2\Gamma_i)_J\right\rangle) \\
&= E_0 && \text{(4a)}\\
&+ \sum_{J_c} E_c(4f^{N-1}\eta(^{2S_f+1}L_f)_{J_f}) \\
&\left\langle \left(\frac{1}{2}, (S_f, L_f)J_f\right)J \middle| \left(\left(\frac{1}{2}, S_f\right)S, L_f\right)J \right\rangle^2 && \text{(4b)}\\
&+ J_{\text{ex}}\left(\frac{(S_f + 1/2)(S_f + 3/2) - S(S+1)}{2}\right) \\
&- \frac{J_{\text{ex}}S_f}{2} && \text{(4c)}\\
&+ E_{\text{cf}}(5d\,^2\Gamma_i) && \text{(4d)}
\end{aligned}$$

It can be seen that: 1) for a fixed 5d crystal-field component 5d $^2\Gamma_i$, we get a set of energy levels which form a pattern with relative energies independent of the 5d crystal-field component as given by (4b-c), i.e., the structure of the pattern is determined purely by the $4f^{N-1}$ core and the high-low spin splitting due to $4f^{N-1}$ and 5d exchange interaction; 2) the shift of the pattern for 5d $^2\Gamma_i (i>1)$ relative to the form for 5d $^2\Gamma_i (i=1)$ is just the energies due to crystal-field splitting given by (4d). The high degeneracy of the energy levels given by Eq. (4) is actually further decreased by other neglected interactions. This effect and the electron-vibration interactions not considered here result into the broad bands in the absorption and excitation spectra measured at room temperature.

We adopt the definition of the electric dipole line strength for the transition between $|Ff\rangle$ and $|Ii\rangle$ given by Reid[1] as:

$$I_q(F, I) = \sum_{f,i} |\langle Ff|D_q|Ii\rangle|^2, \tag{5}$$

where f and i are the partner quantum numbers of F and I to distinguish the degeneracy of transition final and initial states, respectively, and D_q is the qth component of the electric dipole moment.

For transitions between $\left|4f^N\eta_1(^{2S_1+1}L_1)_{J_1}\right\rangle$ and $\left|^{2S_2+1}(4f^{N-1}\eta_2^{2S_f+1}L_f, 5d\,^2\Gamma_i)_{J_2}\right\rangle$ involving isotropic light, the line strength can be written using the results from Duan and Reid[7] and Ning et al.[8] as:

$$\begin{aligned}
&I_{\text{iso}}(\left|4f^N\eta_1(^{2S_1+1}L_1)_{J_1}\right\rangle \leftrightarrow \left|^{2S_2+1}(4f^{N-1}\eta_2^{2S_f+1}L_f, 5d^2\Gamma_i)_{J_2}\right\rangle) \\
&= \frac{1}{3}\sum_{M_1,M_2,\gamma_i,q} \left|\left\langle 4f^N\eta_1(^{2S_1+1}L_1)_{J_1M_1}|D_q|^{2S_2+1}..\right.\right. \\
&\left.\left.\times(4f^{N-1}\eta_2^{2S_f+1}L_f, 5d^2\Gamma_i\gamma_i)_{J_2M_2}\right\rangle\right|^2 \\
&= \delta_{S_1,S_2}\frac{[\Gamma_i]|\langle 4f|r|5d\rangle|^2[J_1][J_2]}{35}\frac{}{[S_1]} \\
&\times \begin{Bmatrix} L_1 & L_f & 3 \\ J_1 & J_2 & S_1 \end{Bmatrix}^2 N[S_1][L_1]\text{cfp}(\eta_1\,^{2S_1+1}L_1; \eta_2\,^{2S_f+1}L_f)^2,
\end{aligned} \tag{6}$$

where $M_i = -J_i, -J_i+1, \ldots, J_i\ (i=1, 2)$, $q=-1, 0, -1$, and γ_i is the partner for the irrep Γ_i; the curly bracket with six numbers is $6j$ symbols for the SO_3 rotation group; $[J]=(2J+1)$; and cfp is the coefficient of fractional parentage. The radial integral $\langle 4f|r|5d\rangle$ can be calculated using the Hartree-Fock method and then corrected for correlation interactions, available from Duan and Reid[18] for all trivalent ions. But usually we are concerned with only the relative intensities, and so the value for $\langle 4f|r|5d\rangle$ is not important. For 4f-5d absorption, it can be seen that from Eq. (6) that: 1) the line strengths for transitions to various final states constructed from the same 5d crystal-field component, when divided by the degeneracy of the 5d crystal-field component, are independent of the detailed 5d crystal-field component, i.e., those transitions form a pattern in the absorption spectra; 2) the same pattern repeats for each 5d crystal-field components but shifts in energy by the 5d crystal-field splitting; 3) the patterns for two 5d crystal-field components may overlap each other due to limited 5d crystal-field splitting.

Experimentally, usually the oscillator strengths, absorption cross sections and spontaneous emission rates are directly measurable instead of the line strength, those quantities are proportional to the line strengths given with Eq. (6), but with coefficients being energy dependent and inversely proportional to the degeneracy of the initial energy level of the transition, which is $(2J_1+1)$ for multiplet $\left|4f^N\eta_1(^{2S_1+1}L_1)_{J_1}\right\rangle$ and $[\Gamma_i]$ $(2J_2+1)$ for multiplet $\left|^{2S_2+1}(4f^{N-1}\eta_2^{2S_f+1}L_f, 5d\,^2\Gamma_i)_{J_2}\right\rangle$. The detailed relations can be found in Reid[1] (Eq. 2.5–2.10) and hence

the data (if corrected for the response of the apparatus) can be easily transformed to line strengths.

RESULTS FOR Nd^{3+} IN A CRYSTAL HOST

The ground and excited configurations for Nd^{3+} are $4f^3$ and $4f^25d$, respectively. The ground multiplet is $^4I_{9/2}$ and the lowest $4f^{N-1}5d$ multiplet is $^4(^3H, 5d\Gamma_i)_{7/2}$. There are many studies on the 4f-5d transitions of Nd^{3+} in crystals.[19–27] The transitions of interest and the available experimental data for 4f-5d transitions are between states of $S=3/2$.

The emission from $^4(^3H, 5d\Gamma_i)_J$ $(J=7/2, 9/2)$ to all the $4f^3$ multiplets with nonzero line strengths are given in Table 1 in units of $[\Gamma_i]|\langle 4f|r|5d\rangle|^2/35$. The values are purely determined by various coupling and recoupling coefficients for SO_3 group (hereafter referred to as by group theory) and hence exact numbers without any rounding errors can be given by fractions. Both exact numbers (in terms of fractions) and floating point values are listed. The displaced energies relative the emission with the largest energy (corresponding to the final $^4I_{9/2}$ multiplet) are also given in column 3 of Table 1. The transitions to $S=1/2$ and $^4S_{3/2}$ are forbidden and hence not listed in the table. The results are plotted in Fig. 1 for the ease of comparison with

TABLE 1 Electric Dipole Line Strengths for Emission from the Two Lowest "Multiplet" of $|4f^2\ (^3H)\ 5d\ SJ_1\rangle$ ($S=3/2$, $J_1=7/2$ or 9/2) to $|4f^3\ SLJ_2\rangle$. The Units are cm^{-1} for Energies, E, and $[\Gamma_i]|\langle 4f|r|5d\rangle|^2/35$ for Line Strengths

^{2S+1}L	J_2	E	7/2		9/2	
^4I	9/2	0	17836/1089	16.4	6860/1089	6.30
	11/2	1862	1960/363	5.40	5120/363	14.1
	13/2	3839	28/99	0.28	686/99	6.93
	15/2	5891	0		8/33	0.24
^4F	3/2	11336	44/21	2.10	22/21	1.05
	5/2	12370	11/7	1.57	7/4	1.75
	7/2	13333	20/63	0.32	35/18	1.94
	9/2	14600	1/63	0.02	65/252	0.26
^4G	5/2	17072	845/147	5.75	21125/6468	3.27
	7/2	17148	2028/539	3.76	4563/1078	4.23
	9/2	18946	507/847	0.60	15795/3388	4.66
	11/2	19353	52/2541	0.02	182/363	0.50
^4D	1/2	28497	44/21	2.10	0	
	3/2	27958	88/63	1.40	176/63	2.79
	5/2	28113	44/147	0.30	256/147	1.74
	7/2	30212	8/441	0.02	100/441	0.23

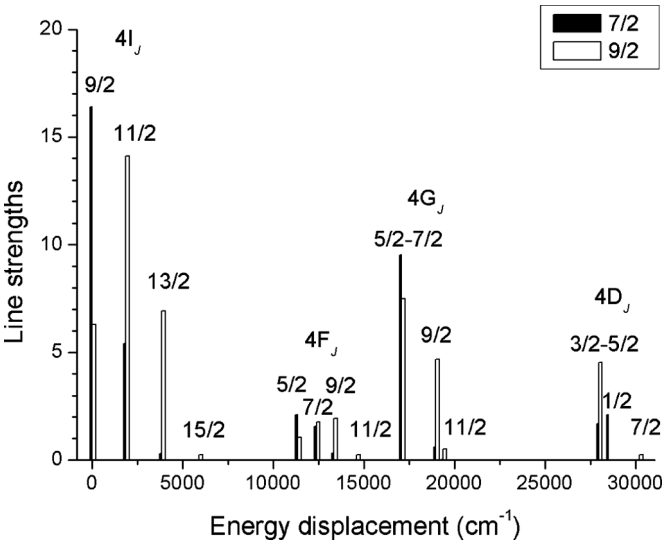

FIGURE 1 d-f emission for Nd^{3+} in the strong 5d crystal-field case. The emission to the ground state $^4I_{9/2}$ has the highest energy. The energy displacement is given as the difference between the emission energy for emission to $^4I_{9/2}$ and the emission energy for emission to the considered multiplet. The line strengths are the values in Table 1, in units of $[\Gamma_i]|\langle 4f|r|5d\rangle|^2/35$.

the measured spectra. It is noted that measured spectra are usually relative decay rates or emission intensity, which are proportional to the cube or fourth power of emission energy multiplied by the line strengths.

For a given 5d crystal-field component, the positions of $S=3/2$ multiplets $4f^25d$, i.e., the energy of $^4(4f^2\ ^3L_f, 5d\ ^2\Gamma_i)_{J_2}$, can be given relative to $^4(4f^2\ ^3H, 5d\ ^2\Gamma_i)_{7/2}$ as in Table 2. The results are also plotted in Fig. 2 for the ease of comparison with absorption spectra. It is noted that measured spectra usually

TABLE 2 The Energies of High-Spin $4f^2$ Core Multiplets and the High-Spin $4f^25d$ Multiplets (Units: cm^{-1})

$4f^2$ core	Energy	$4f^25d$	Energy	
$^3H_4$	0	$^4(^3H, 5d\Gamma)$ 7/2	$E(^3H_4)$	0
$^3H_5$	2672	$^4(^3H, 5d\Gamma)$ 9/2	$[2\ E(^3H_4)+3\ E(^3H_5)]/5$	1603
$^3H_6$	5423	$^4(^3H, 5d\Gamma)$ 11/2	$[13\ E(^3H_5)+5E(^3H_5)]/18$	3436
		$^4(^3H, 5d\Gamma)$ 13/2	$E(^3H_6)$	5423
$^3F_2$	5521	$^4(^3F, 5d\Gamma)$ 3/2	$E(^3F_2)$	5521
$^3F_3$	7298	$^4(^3F, 5d\Gamma)$ 5/2	$[4\ E(^3F_2)+5\ E(^3F_3)]/9$	6508
$^3F_4$	7787	$^4(^3F, 5d\Gamma)$ 7/2	$[3\ E(^3F_3)+E(^3F_4)]/4$	7420
			$E(^3F_4)$	7787
$^3P_0$	23204	$^4(^3P, 5d\Gamma)$ 1/2	$[2\ E(^3P_0)+E(^3P_1)]/3$	23453
$^3P_1$	23980	$^4(^3P, 5d\Gamma)$ 3/2	$[5\ E(^3P_1)+E(^3P_2)]/6$	24239
$^3P_2$	25535	$^4(^3P, 5d\Gamma)$ 5/2	$E(^3P_2)$	25535

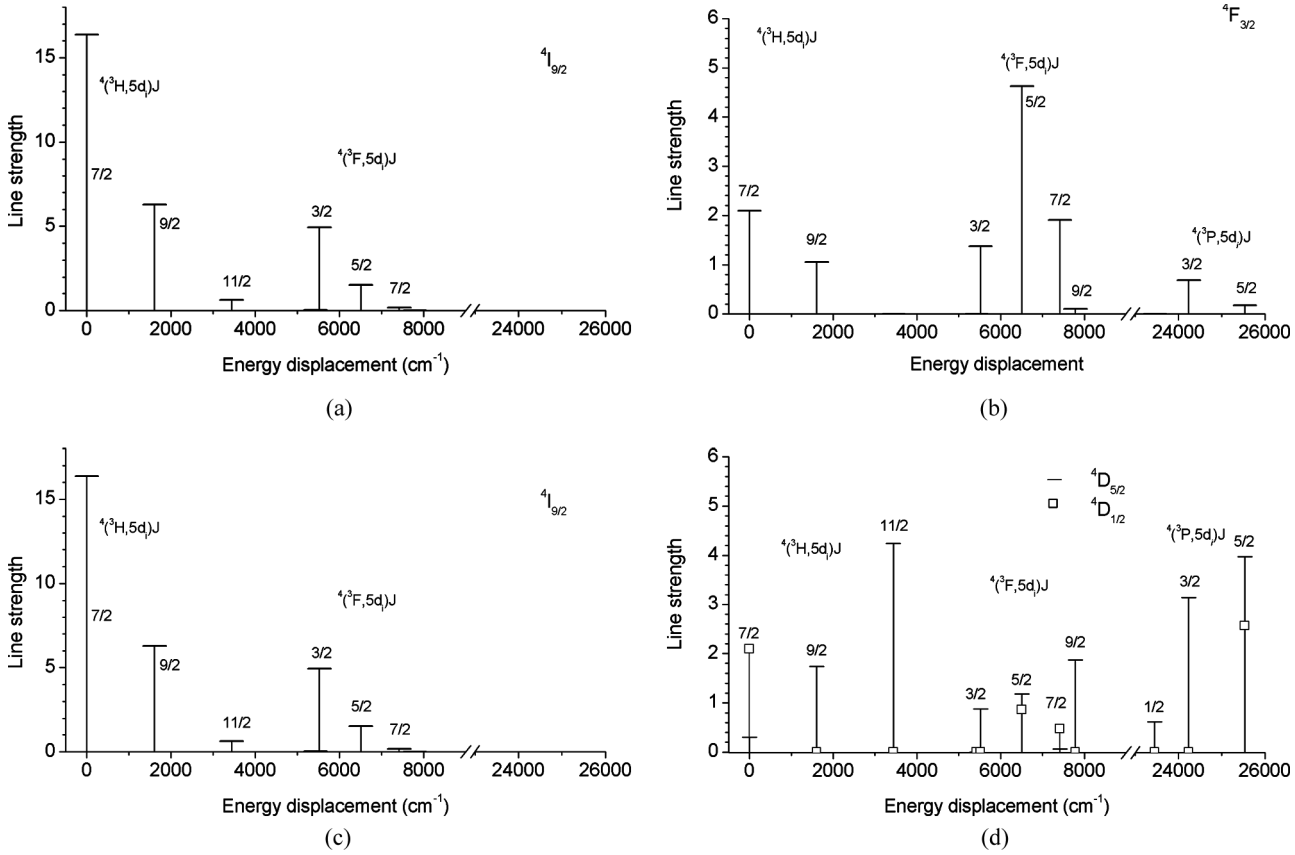

FIGURE 2 **Line strengths for ground and excited state absorption to various $4f^25d$ multiplets of a specific 5d crystal-field component. The initial states for the spectra are: (a) $^4I_{9/2}$, (b) $^4F_{3/2}$, (c) $^4D_{3/2}$ and (d) $^4D_{5/2}$ and $^4D_{1/2}$. The final $4f^25d$ states are given in the figures. The energies are given relative to that of the lowest $4f^25d$ state. It is noted that: 1) intensities in the experimental spectra need to be converted to line strengths for comparison with the plots given here; 2) experimental spectra usually contain transitions to several (up to 5) 5d crystal-field components.**

represent absorption cross sections, which are proportional to the product of photon energies with the line strengths.

The ground state absorption (GSA) and excited state absorption of Nd^{3+} in $LiYF_4$ have been studied. Here we calculate the absorption from the ground state ($^4I_{9/2}$) and ESA from quasi-stable multiplet $^4F_{3/2}$ and ^4D_J ($J=3/2$, 5/2 and 1/2 in increasing energy order). The results are also purely determined by group theory and can also be given in exact numbers (fractions) without rounding errors.

COMPARISON WITH EXPERIMENTAL SPECTRA FOR Nd^{3+} IN CRYSTALS

The emissions from the lowest $4f^25d$ states of Nd^{3+} in $LiYF_4$ and YPO_4 have been measured and simulated by Peijzel et al. in Figures 4 and 5 of Peijzel et al.[26] The intensity for the peak with final state $^4I_{11/2}$ is about 1/3 of the intensity for $^4I_{9/2}$, and the peak with final state $^4I_{13/2}$ is weaker than that for $^4I_{9/2}$ by about two orders of magnitude. The relative emission intensities for Nd^{3+} in the two crystals $LiYF_4$ and YPO_4 are almost the same, except for the vibronic structure, which is not simulated here. The experimental results are comparable with the calculated line strengths given in Table 1. The emission spectrum from the lowest $4f^25d$ state to ^4I_J, ^4F_J and ^4G_J was given by van Pieterson et al. (see Figure 1 of van Pieterson et al.[22]) for Nd^{3+} in $LiYF_4$, and by Librantz et al.[21] for Nd^{3+} in BaY_2F_8 and $LiYF_4$. The intensity patterns for those spectra are the same regardless of the crystals as predicted in this paper. Due to uncertainty on the corrections for detection responses, an exact comparison of our theoretical results with their experimental ones may not be sensible, but it can seen that the calculated ratios of line strengths, 33/182 and 45/98 for 4F/4I and 4G/4I, respectively, are compatible with the measured relative intensities.

The ground and excited state absorptions of Nd^{3+} in $LiYF_4$ have been measured by Collombet et al.[23] and Malkin et al.[27] together with theoretical simulations utilizing the full crystal-field Hamiltonian.

The absorption from the ground state is given with high resolution in the Figure 7 of Ref.[27] Both the measured and calculated absorption to first 5d crystal-field component in the Figure 7 of Malkin et al.[27] contain two bands. One of these starts at *ca.* 56500 cm^{-1} with a shoulder at around 1600 cm^{-1} higher in energy and of *ca.* 1/3 in relative intensity. The other band starts at *ca.* 62000 cm^{-1} with intensity of about the same or less than 1/3 of that of the first 4f-5d band. Our theoretical results in Table 3 assign the peak at 56500 cm^{-1} and the shoulder to absorption from the ground multiplet $^4I_{11/2}$ to $^4(^3H, 5d_1)J, J=7/2$ and 9/2, respectively, with shift of 1603 cm^{-1}. The 62000 cm^{-1} band is assigned to the absorption to $^4(^3F, 5d_1)$ *J*, $J=3/2$. The experimental and predicted shift are *ca.* 5500 cm^{-1} and 5521 cm^{-1}, respectively. The broad peaks at 64500 cm^{-1} and 70000 cm^{-1} are then assigned to the absorptions to $^4(^3H,5d_2)$ *J* ($J=7/2$ and 9/2) and $^4(^3F, 5d_2)$ *J* ($J=3/2$), respectively. This assignment gives an experimental $E_{cf}(5d_2)$-$E_{cf}(5d_1)=$ 8000 cm^{-1} and $^4(^3F,5d_2)_{3/2}$-$^4(^3H,5d_2)_{9/2}=5500\ cm^{-1}$. Those two broad peaks can be considered as a repeat of the pattern similar to the one due to the absorption to the first 5d crystal-field component, but with much broader line widths. The much-broader linewidths are due to much stronger ionization of the second 5d crystal-field component to the conduction band. There are some more even-broader bands in the measured absorption spectra, which can be assigned to absorption to higher 5d crystal-field components by following the same principal.

The absorption from $^4F_{3/2}$ to $^4(^3F, 5d_1)_J=5/2$ is calculated to be more than twice the intensity of that to $^4(^3H, 5d_1)J=9/2$ and also of energy *ca.* 6500 cm^{-1} higher. The measured excited-state absorption spectra from $^4F_{3/2}$ are very broad, so only the line strength ratio of the convolution of $^4(^3H, 5d_1)$ *J* ($J=7/2$–13/2) and that of the $^4(^3F, 5d_1)$ ($J=3/2$–9/2) can be given, which is about 0.38, and comparable to the theoretical line strength ratio 11/28 obtained from data listed in Table 3. The intensities for the excited state absorption from ^4D_J to $4f^25d$ states are calculated and shown in Table 3. It is noted that, since the splitting between $J=3/2$ and 5/2 is

TABLE 3 Electric Dipole Line Strengths for Ground and Excited State Absorption to Various $4f^25d$ "Multiplets" $^{2S_1+1}(4f^2\ SL)\ J_1$

Final state			Initial state of absorption						
$^{2S_1+1}(4f^2SL, 5d)$	J_1	E (cm^{-1})	$^4I_{9/2}$ (0 cm^{-1})		$^4F_{3/2}$ (11336 cm^{-1})		$^4D_{3/2}$ (27958 cm^{-1})	$^4D_{5/2}$ (28113 cm^{-1})		$^4D_{1/2}$ (28497 cm^{-1})	
$^4(^3H,5d_i)$	7/2	0	17836/1089	16.4	44/21	2.10	88/63	1.40	44/147	0.30	44/21	2.10
	9/2	1603	6860/1089	6.30	22/21	1.05	176/63	2.80	256/147	1.74		
	11/2	3436	1008/1573	0.64					208/49	4.25		
	13/2	5423	70/4719	0.015								
$^4(^3F,5d_i)$	3/2	5521	104/21	4.95	48/35	1.37	32/35	0.91	216/245	0.88	0	
	5/2	6508	117/77	1.52	162/35	4.63	3/35	0.086	289/245	1.18	6/7	0.86
	7/2	7420	130/693	0.12	40/21	1.91	80/63	1.27	10/147	0.068	10/21	0.48
	9/2	7787	5/693	0.007	2/21	0.095	25/63	0.40	275/147	1.87		
$^4(^3P,5d_i)$	1/2	23453			0		0		30/49	0.61	0	
	3/2	24239			24/35	0.69	36/35	1.03	768/245	3.14	0	
	5/2	25535			6/35	0.17	144/35	4.11	972/245	3.97	18/7	2.57

very small, the thermal occupation of $J=5/2$ is not negligible at room temperature, and so the absorption line strength is a weighted sum of the absorption from $J=3/2$ and $J=5/2$. In general, we have:

$$I_{\mathrm{iso}}(T) = \frac{\sum_i g_i \exp(-E_i/k_BT)(I^i_{\mathrm{iso}}/g_i)}{\sum_i g_i \exp(-E_i/k_BT)} \propto \sum_i \exp(-E_i/k_BT) I^i_{\mathrm{iso}}, \quad (7)$$

where T is the temperature, g_i is the degeneracy for the energy level with energy E_i, and k_B is the Boltzmann constant. It is noted that when absorption cross-section, etc. are calculated, the degeneracy factor is no longer dividable, since it has been taken into account in Eq. (7) already. For the case of $^4D_{3/2,\ 5/2}$ we have

$$I_{\mathrm{iso}}(300\mathrm{K}) = 0.143 I^{(3/2)}_{\mathrm{iso}} + 0.068 I^{(5/2)}_{\mathrm{iso}}. \quad (8)$$

However, the available measured spectra do not allow a sensible comparison between the calculations here with the measurement. So Eq. (8) is given here mainly for later reference.

CONCLUSIONS

The energy level structure and 4f-5d ground-state and excited-state absorption and 5d-4f emission line strengths have been calculated for the usual case that the 5d crystal-field interaction is much stronger than the 4f-5d Coulomb interaction and 4f spin-orbital interaction. It has been shown that for absorptions and emissions, by neglecting the usually negligible mixing of different spectrum term $^{2S_f+1}L_f$ (S_f and L_f being total spin and orbital angular momentum quantum numbers, respectively), the line strengths of transitions to or from a given 5d crystal-field component are purely determined by coupling and recoupling coefficients of SO_3 group (irrelevant of the actual point group in question), and are hence independent of the host lattice. The results have been used to interpret the measured data for Nd^{3+} in various crystals.

ACKNOWLEDGEMENTS

Financial support for this work under the National Science Foundation of China (grant Nos. 10874173 and 10874253) is gratefully acknowledged.

REFERENCES

1. Liu, G. K. Electronic energy level structure. Reid, M. F., transition intensities. In *Spectroscopic Properties of Rare Earths in Optical Materials*; Liu, G. K. and Jacquier, B. Eds.; Springer-Verlag: Berlin, 2005; 1–126.
2. Burdick, G. W.; Reid, M. F. $4f^n$–$4f^{n-1}5d$ transitions. In *Handbook on the Physics and Chemistry of Rare Earths*; Gschneidner, K. A., Jr.; Bünzli, J.-C. G.; Pecharsky, V. K., Eds.; Elsevier B.V: Amsterdam, 2007, Vol. 37, 61–98.
3. Ogasawara, K.; Watanabe, S.; Toyoshima, H.; Brik, M. G. Chapter 231. First-principles calculations of $4f^n \rightarrow 4f^{n-1}5d$ transition spectra. In *Handbook on the Physics and Chemistry of Rare Earths*; Gschneidner, K. A. Jr.; Bünzli, J.-C. G.; Pecharsky, V. K., Eds.; Elsevier B.V: Amsterdam, 2007, Vol. 37, 1–59.
4. van Pieterson, L.; Reid, M. F.; Burdick, G. W.; Meijerink, A. $4f^n \rightarrow 4f^{n-1}5d$ transitions of the heavy experiment and theory lanthanides. *Phys. Rev. B* **2002**, *65*, 045114.
5. van Pieterson, L.; Reid, M. F.; Wegh, R. T.; Soverna, S.; Meijerink, A. $4f^n \rightarrow 4f^{n-1}5d$ transitions of the light Experiment and theory lanthanides. *Phys. Rev. B* **2002**, *65*, 045113.
6. Malkin, B. Z.; Solovyev, O. V.; Malishev, A. Yu.; Saikin, S. K. Theoretical studies of electron-vibrational $4f^N$–$4f^{N-1}5d$ spectra in $LiYF_4$: Re^{3+} crystals. *J. Lumin.* **2007**, *125*, 175–183.
7. Duan, C. K.; Reid, M. F. A simple model for f → d transitions of rare-earth ions in crystals. *J. Solid State Chem.* **2003**, *171*(1–2), 299–303.
8. Ning, L. X.; Duan, C. K.; Xia, S. D.; Reid, M. F.; Tanner, P. A. A model analysis of $4f^N$–$4f^{N-1}5d$ transitions of rare-earth ions in crystals. *J. Alloy. Compd.* **2004**, *366*(1–2), 34–40.
9. Xia, S. D.; Duan, C. K.; Deng, Q.; Ruan, G. Assignment of 4f → 5d excitation spectra of Nd^{3+} in crystals using the simple model. *J. Solid State Chem.* **2005**, *178*(9), 2643–2646.
10. Xia, S. D.; Duan, C. K. Extension of a simple model for f-d transition and applications to reassignment of excitation spectra of Ho^{3+}-doped crystals. *Chin. Phys. Lett.* **2005**, *22*(10), 2680–2683.
11. Xia, S. D.; Chen, T.; Duan, C. K. Interpretation of the 4f-5d excitation spectra of Eu^{3+} and Tb^{3+} doped in crystals. *J. Rare Earths* **2006**, *24*(4), 400–407.
12. Xia, S. D.; Duan, C. K. The simple model and its application to interpretation and assignment of 4f-5d transition spectra of rare-earth ions in solids. *J. Lumin.* **2007**, *122*, 1–4.
13. Duan, C. K.; Xia, S. D.; Reid, M. F.; Ruan, G. Study of the f → d transition of heavy lanthanide and actinide ions in crystals using the simple model. *Phys. Status Solidi B* **2005**, *242*(12), 2503–2508.
14. Ma, C. G.; Reid, M. F.; Duan, C. K.; Xia, S. D.; Yin, M. Recent advances in simple model for 4f-5d transitions of lanthanide ions in solids. *J. Rare Earths* **2007**, *25*, 262–267.
15. Reid, M. F.; Duan, C. K.; Zhou, H. Crystal-field parameters from *ab initio* calculations. *J. Alloys Compd.* **2009**, doi:10.1016/j.jallcom.2008.12.004.
16. Gorller-Walrand, C.; Binnemans, K. Rationalization of crystal-field parameterization. In *Handbook on the Physics and Chemistry of Rare Earths*; Gschneidner, K. A. Jr.; Eyring, L.; Elsevier Science B.V.: Amsterdam, 1996; Chap. 23, 121–283.
17. Reid, M. F.; van Pieterson, L.; Meijerink, A. Trends in parameters for the $4f^N \leftrightarrow 4f^{N-1}5d$ spectra of lanthanide ions in crystals. *J. Alloys Compd.* **2000**, *344*, 240.
18. Duan, C. K.; Reid, M. F. General calculation of 4f-5d transition rates for rare-earth ions using many-body perturbation theory. *J. Chem. Phys.* **2005**, *122*, 094714.
19. Thøgersen, J.; Gill, J. D.; Haugen, H. K. Stepwise multiphoton excitation of the $4f^25d$ configuration in Nd^{3+}:YLF. *Opt. Commun.* **1996**, *132*, 83–88.
20. Dooley, P. W.; Thøgersen, J.; Gill, J. D.; Haugen, H. K.; Brooks, R. L. Studies of two-photon excitation and vacuum ultraviolet fluorescence in Nd:YLF. *Opt. Commun.* **2000**, *183*, 451–459.

21. Librantz, A. F. H.; Gomes, L.; Tarelho, L. V. G.; Ranieri, I. M. Investigation of the multiphoton excitation process of the $4f^2 5d$ configuration in $LiYF_4$ and $LiLuF_4$ crystals doped with trivalent neodymium ion. *J. Appl. Phys.* **2004**, *95*, 1681–1691.
22. van Pieterson, L.; Wegh, R. T.; Meijerink, A.; Reid, M. F. Emission spectra and trends for $4f^{n-1}5d$ transitions of lanthanide ions, Experiment and theory. *J. Chem. Phys.* **2001**, *115*, 9382–9392.
23. Collombet, A.; Guyot, Y.; Joubert, M. F.; Laroche, M.; Margerie, J.; Moncorgé, R.; Descroix, E. Experimental and theoretical investigation of $4f^3$-$4f^2 5d$ interconfigurational transitions in Nd^{3+}: $LiYF_4$ crystals. *Phys. Rev. B* **2003**, *68*, 035115.
24. Librantz, A. F. H.; Gomes, L.; Baldochi, S. L.; Ranieri, I. M.; Britob, G. E. Luminescence study of the $4f^2 5d$ configuration of Nd^{3+} in $LiYF_4$, $LiLuF_4$ and BaY_2F_8 crystals. *J. Lumin.* **2006**, *121*, 137–148.
25. Gusowski, M. A.; Ryba-Romanowski, W. Inter- and Intraconfigurational Transitions of Nd^{3+} in Hexafluorocryolite-type K_3YF_6 Lattice. *J. Phys. Chem. C* **2008**, *112*, 14196–14201.
26. Peijzel, P. S.; Vergeer, P.; Meijerink, A.; Reid, M. F.; Boatner, L. A.; Burdick, G. W. $4f^{n-1}5d$-$4f^n$ emission of Ce^{3+}, Pr^{3+}, Nd^{3+}, Er^{3+}, and Tm^{3+} in $LiYF_4$ and YPO_4. *Phys. Rev. B* **2005**, *71*, 045116.
27. Malkin, B. Z.; Solovyev, O. V.; Malishev, A. Yu.; Saikin, S. K. Theoretical studies of electron-vibrational $4f^N$-$4f^{N-1}5d$ spectra in $LiYF_4$: RE^{3+} crystals. *J. Lumin.* **2007**, *125*, 175–183.